Chapter 5
Material Characterization of Pin-Core Latex Polymer Foam Under Static and Dynamic Loads

K. Venkataramana, R. K. Singh, Anindya Deb, Vivek Bhasin, K. K. Vaze and H. S. Kushwaha

Abstract Cellular polymer foams find extensive applications as energy absorbers under static, impact and blast loads due to their capacity to absorb energy under constant stress up to full densification strain (Ashby et al. Metal foams: a design guide. Butterworth-Heinemann, Oxford, 2000 [1]; Gibson and Ashby, Cellular solids: structure and properties. Cambridge University Press, Cambridge, 1999 [2]). In the present paper, the material characterization of natural latex cellular polymer foam used in the field air blast experiments (Venkataramana et al. Proc Eng 173:547–554, 2017 [3]; Venkataramana et al. Numerical simulation of blast wave mitigation using foam impregnated with water. DAE BRNS Symposium on Multiscale Modeling of Materials and Devices (MMMD-2014), 2014 [4]) performed to assess the blast mitigation effect of fluid-filled open-cell pin-core polymer foam is presented. Static compression tests were performed to study the quasi-static behavior of the pin-core latex polymer foam. The Ogden hyper-elastic material parameters are determined from the analysis of static compression test data using ADINA (automatic dynamic incremental nonlinear analysis) v 9.2, ADINA R&D, Inc., Watertown [5]). Further, results of the static compression tests on dry foam and water-saturated foam are compared and discussed. In addition, the dynamic behavior of the pin-core latex cellular foam is investigated by conducting drop tower impact experiment and numerical simulation of the drop tower experiment using LS-DYNA (LS-DYNA v971, Livermore Software Technology Corporation, Livermore [6]). The stress–time history from the drop tower experiment is compared with that of simulation, and good correlation is found between the two sets of results.

Keywords Blast protection · Fluid-filled foam · Blast waves · Polymer foam · High explosive · Near-field blast

K. Venkataramana (✉) · V. Bhasin
Reactor Safety Division, BARC, Mumbai 400085, India
e-mail: kvr_suru@yahoo.com

R. K. Singh · K. K. Vaze · H. S. Kushwaha
Raja Ramanna Research Fellow, DAE, BARC, Mumbai 400085, India

A. Deb
CPDM, Indian Institute of Science (IISc), Bengaluru 560012, India

M. Vinyas et al. (eds.), *Advances in Structures, Systems and Materials*,
Lecture Notes on Multidisciplinary Industrial Engineering,
https://doi.org/10.1007/978-981-15-3254-2_5

5.1 Introduction

Cellular polymer foams consist of a three-dimensional array of interconnected cells with solid cell walls and cell faces. When the cell faces are open, they are called open-celled foams, and when the cell faces are closed, they are called closed-cell foams. The cellular polymer foams are characterized by their relative density defined as (ρ^*/ρ_s), where ρ^* is the overall density of the foam, and ρ_s is that of the solid of which the foam is made. The relative density of foams varies from less than 0.3 to as low as 0.003. The porosity of the foam is defined as $1 - (\rho^*/\rho_s)$. Low-density open-cell polymer foams have porosity up to 0.97. The densification strain for open-cell elastomeric polymer foams is given by [2] $\varepsilon_D = 1 - 1.4(\rho^*/\rho_s)$. Flexible polymer foams such as open-cell latex polymer foam absorb energy by elastic bending and buckling of cell walls and release the energy after the load is removed. Though their use as energy absorbers under static and low-velocity impact loads in automobile and packaging industry is well known, low-density open-cell polymer foams have also drawn the attention of researchers for military applications as energy absorbers under blast and impact loads [7–10]. Dawson [7] analyzed the fluid-filled open-cell polymer foam for blast mitigation, and Venkataramana et al. [3, 4, 11] have experimentally and numerically investigated the application of open-cell natural latex polymer foam filled with fluid for mitigating the close-range air blast effects on structures. However, the material properties of the pin-core latex polymer foam used in the blast experiments are not available in open literature.

Typical compositions and manufacturing methods of the pin-core natural latex polymer foam are discussed by Rani (Chap. 9) in Ref. [12]. The natural latex pin-core open-cell polymer foam used in the current experiments is manufactured by MM foam Ltd. [13]. The foam is categorized as low-density elastomeric cellular polymer foam with an overall density of 20 kg/m^3, relative density (ρ^*/ρ_s) of 0.022 and 97.8% porosity. This paper presents results of static compression tests and drop tower impact experiments performed to characterize the open-cell pin-core latex polymer foam under static and dynamic loading conditions. In addition, numerical simulations of the static compression tests and drop tower impact experiments are performed, and the simulation results are compared with the experimental data.

5.2 Drop Tower Experiment on Foam

The drop tower experiments were performed on a miniature drop tower, which is a small-scale drop tower designed to perform experiments on soft materials like polymer foams. The drop tower experimental setup is shown in Fig. 5.1. Drop tower tests were conducted on 100 mm thick foam block of base size 150 mm × 150 mm. The drop weight is allowed to fall freely under gravity on the foam block from a predetermined height. The impact of the drop weight imparts an initial velocity $V_0 = \sqrt{2gh}$ to the top surface of the foam block. The force–time history acting

Fig. 5.1 Experimental setup for drop tower experiment on foam block of 150 mm × 150 mm × 100 mm

on the foam block is acquired by the data acquisition system attached to the drop tower. The force–time history (Fig. 5.2) is converted into acceleration–time history and then is integrated twice to get the displacement–time history of the foam block. The displacement–time history is used to calculate the strain–time history developed in the foam and finally the dynamic stress–strain curve is derived. The experimental dynamic stress–strain response of the foam is shown in Fig. 5.3 which shows a 0.26 MPa stress at 19% strain.

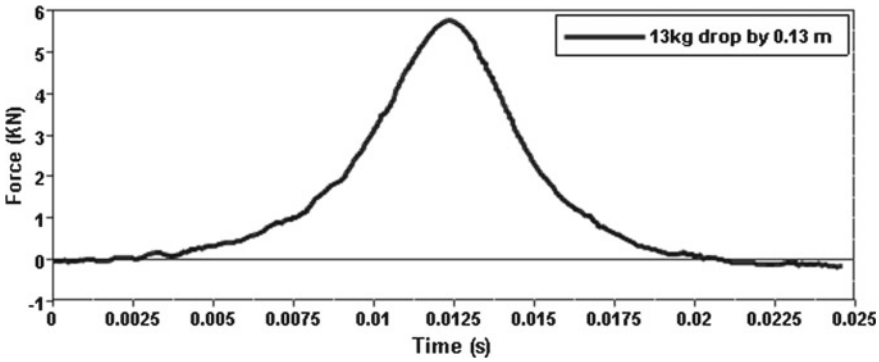

Fig. 5.2 Force–time history, with time from the point of contact between the drop weight and the foam

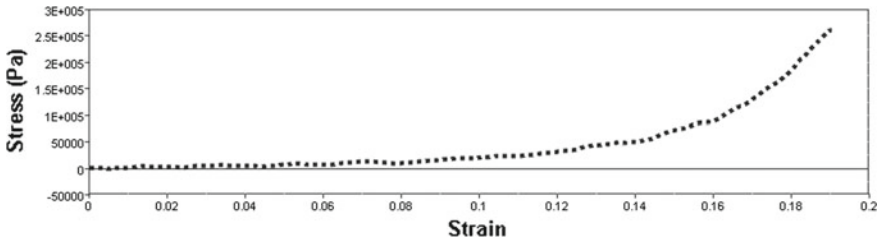

Fig. 5.3 Experimental dynamic stress–strain curve of foam block for up to 19% strain

5.2.1 Simulation of Drop Tower Experiment

Simulations of the drop tower experiments are performed with LS-DYNA [6] code. The simulation setup is shown in Fig. 5.4. The foam block and the drop weight are meshed with brick elements. The bottom of the foam block is fixed in all degrees of freedom. The drop weight is modeled as an elastic steel plate. In order to simulate the experimental conditions, the plate is given an initial velocity corresponds to the velocity acquired by the free-falling mass, $V = \sqrt{2gh}$. The interaction of the plate with the foam block is enforced by surface-to-surface contact algorithm in LS-DYNA. The dynamic behavior of the foam is modeled by MAT_FU_CHANG_FOAM material model (Mat_083) available in LS-DYNA. This material model is suitable to model dynamic compressive behavior of low-density foams, and it allows the stress–strain curves from drop tower experiments to be directly used as input to LS-DYNA material model. The stress–strain values of the foam derived from the drop tower experiment are given as input for the FU_CHANG_FOAM material model [14]. The LS-DYNA program internally calculates the other material parameters using the input test data. The force–time history from the drop tower experiment is converted into stress–time history and compared with that of simulation shown in Fig. 5.5. It is seen that there is a good agreement between the experimental and simulated stress–time history.

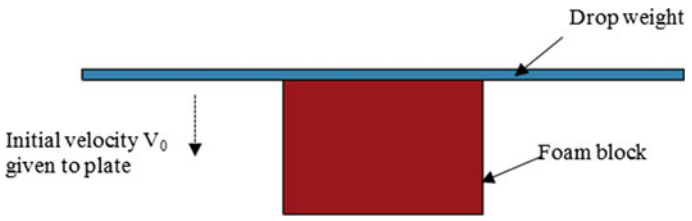

Fig. 5.4 Simulation of drop tower test using LS-DYNA

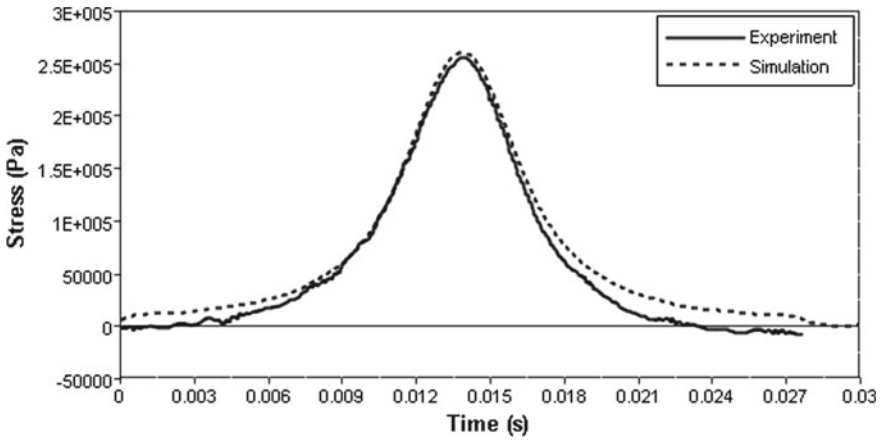

Fig. 5.5 Normal stress–time response of the foam block for 0.13 m height fall of drop weight of 13 kg

5.3 Static Compression Tests on Foam

The foam block used in the actual blast experiments is 100 mm in thickness. The foam is made from natural latex using pin-core method of manufacturing. The pin-core method introduces uniformly distributed cylindrical holes of approximately 5 mm diameter in the foam block. Foam specimens of full thickness (100 mm thick) of foam block used in the field air blast experiments are used in the static compression tests in order to determine the properties of the material in conditions as close as possible to the actual field conditions in which the foam is used. The test specimen is of square base size 150 mm × 150 mm and 100 mm thickness. The specimen size is greater than the minimum size (50 mm × 50 mm base and 25 mm thickness) recommended by the ASTM standard D3574-11 [15] for compression testing of flexible polymer foams. Figure 5.6 shows the natural latex polymer pin-core foam used in the field

Fig. 5.6 Natural latex pin-core polymer foam used in the field air blast experiments [3, 11]

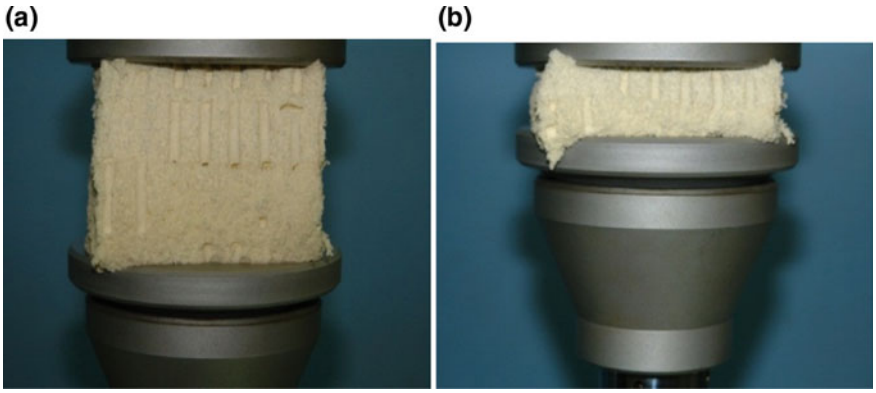

Fig. 5.7 Dry foam testing **a** foam at initial condition and **b** foam at 95% compression

Table 5.1 Summary of compression tests performed on dry foam

Test no.	Compression stroke length (mm)	Crosshead speed (mm/s)	Peak force (N)	Original thickness of foam specimen (mm)
1	95	10	2173	100
2	95	20	1980	100
3	94.2	40	1688	100

air blast experiments. The foam specimen during the compression test is shown in Fig. 5.7.

The uniaxial compression tests were performed at various crosshead speeds. Table 5.1 summarizes the compression tests performed on the dry foam. Figure 5.8 shows the compressive stress–strain response of the dry foam. There was no permanent set observed in the compression test. The foam block completely recovered its initial shape on removal of the load. The foam thus remained elastic during one static uniaxial compression loading and unloading cycle.

As it can be seen from Table 5.1, as the crosshead speed is increased from 10 mm/s to 40 mm/s, the peak load is decreased from 2173 to 1688 N and a 22% reduction in peak-load-carrying capacity at 95% compression. This reduction of peak load may be attributed to early crushing of cell walls at high crosshead speeds (high strain rates). When the foam is loaded slowly, the foam cells get enough time to come to equilibrium with the applied load till peak load is reached, whereas at higher crosshead speeds, early crushing of the foam cell walls results in reduction in the peak-load-carrying capacity of the foam.

Compression tests were also performed on foam fully saturated with water, and the corresponding stress–strain response is compared with that of dry foam in Fig. 5.9. It has been observed that water in the pores of the foam contributed to the load-carrying capacity of the foam. Peak stress in the dry foam is observed to be 96,489,

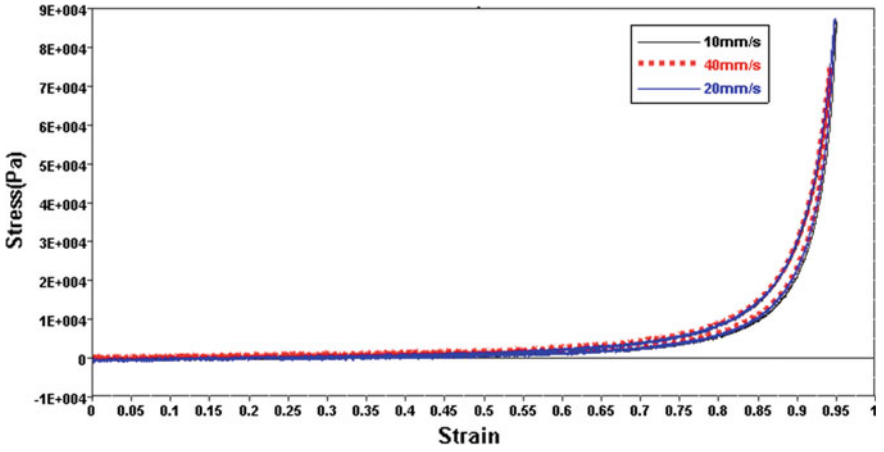

Fig. 5.8 Experimental stress–strain curves of foam at crosshead speeds of 10, 20 and 40 mm/s (corresponding strain rates are 0.1 s^{-1}, 0.2 s^{-1}, and 0.4 s^{-1}, respectively). The peak stress at 40 mm/s crosshead speed is less than the peak stress at 10 and 20 mm/s speed

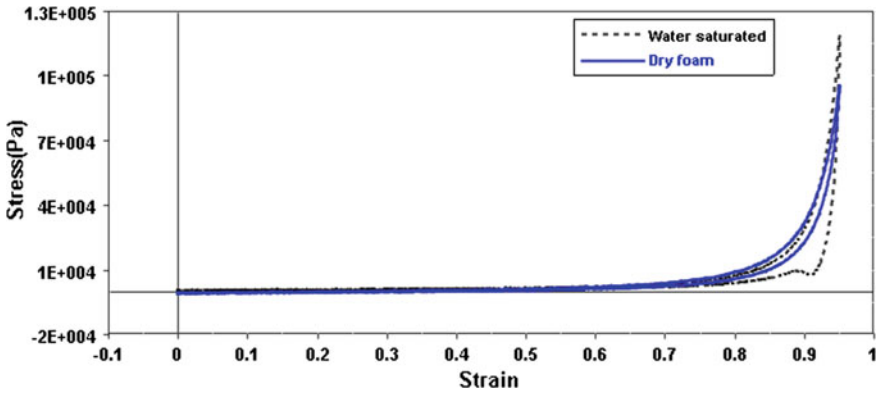

Fig. 5.9 Comparison of experimental stress–strain curves of foam at crosshead speeds of 10 mm/s (strain rates are 0.1 s^{-1}), for dry foam and water-saturated foam

and 118,489 Pa in water-saturated foam, an increase of 22.8% with the presence of water in the pores. This increase in strength is due to the additional work required to expel the fluid (water) from the foam during its compression [4]. It is further observed from Fig. 5.9 that the unloading curve is steeper for the water-saturated foam, with the stress decreasing rapidly at almost constant strain.

This is due to the loss of elasticity of the foam in the presence of water during the unloading cycle as the foam remained at maximum strain like a perfectly plastic material until the load is almost completely removed. The sudden change in the slope in the unloading curve shown in Fig. 5.9 is due to the sudden elastic recovery of the foam at the end of unloading cycle, when the load is almost removed. The

compression tests with water-saturated foam were repeated, and they gave the same stress–strain curve as shown in Fig. 5.9.

5.4 Simulation of Static Compression Tests

The static uniaxial compression tests on the dry foam are simulated using ADINA [5] finite element software. The 150 mm × 150 mm × 100 mm^3 test specimen is represented by a plane strain model. The bottom support and the top plate are treated as rigid surfaces. Frictionless contact between the foam and the supports is assumed. The top rigid plate is given downward displacement corresponding to the compression stroke during the uniaxial compression experiment. The problem is solved in small time steps considering the material and geometric nonlinearities.

5.4.1 Material Model

The dry foam is modeled with Ogden hyper-elastic material model [5] with its parameters determined from the uniaxial compression experimental data. Ogden material model is based on the following expression for strain energy density (i.e., strain energy per unit volume) [16]:

$$W_{\mathrm{D}} = \sum_{n=1}^{9} \left(\frac{\mu_n}{\alpha_n} \left[\lambda_1^{\alpha_n} + \lambda_2^{\alpha_n} + \lambda_3^{\alpha_n} - 3 \right] \right) \mathrm{N/m^2} \tag{5.1}$$

where μ_n and α_n are the Ogden material constants and λ_i's are the square roots of the principal stretches of the Cauchy–Green deformation tensor. Choosing only μ_n, $\alpha_n \neq 0$, n = 1, 2, 3, the standard three-term Ogden material description is recovered from the general model given by Eq. (5.1). The Ogden material model coefficients are determined by least-squares fit between the test data and the strain energy density function. The coefficients determined using ADINA for the latex polymer foam are given in Table 5.2, and the curve fit to compression experimental data is shown in Fig. 5.10.

Table 5.2 Ogden material model parameters for the natural latex pin-core cellular polymer foam

μ parameter	Value (N/m^2)	α parameter	Value
μ_1	681.5047	α_1	1.3
μ_2	11.45471	α_2	6.3
μ_3	43.09203	α_3	−2.5

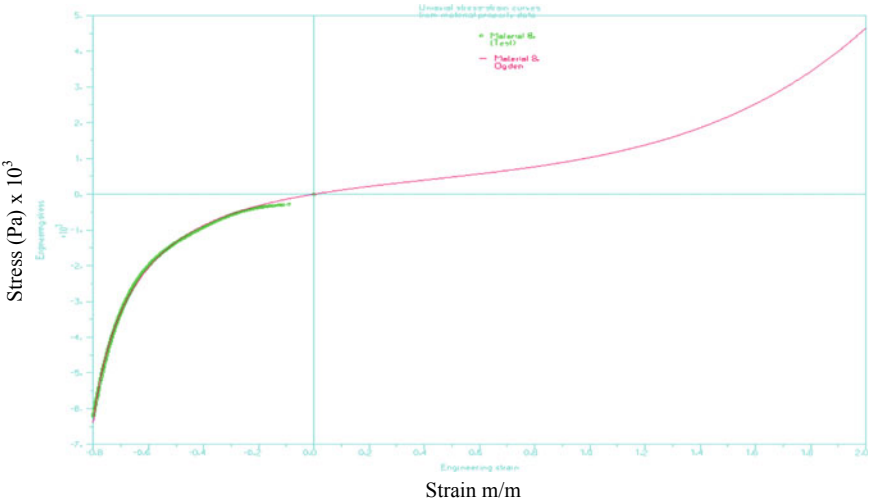

Fig. 5.10 Curve fit to the latex polymer foam compression test data in ADINA

Using the Ogden material parameters from Table 5.2, the stress–strain curves of the foam material from the UTM compression test and the simulation are shown in Fig. 5.11 which shows good agreement between the two.

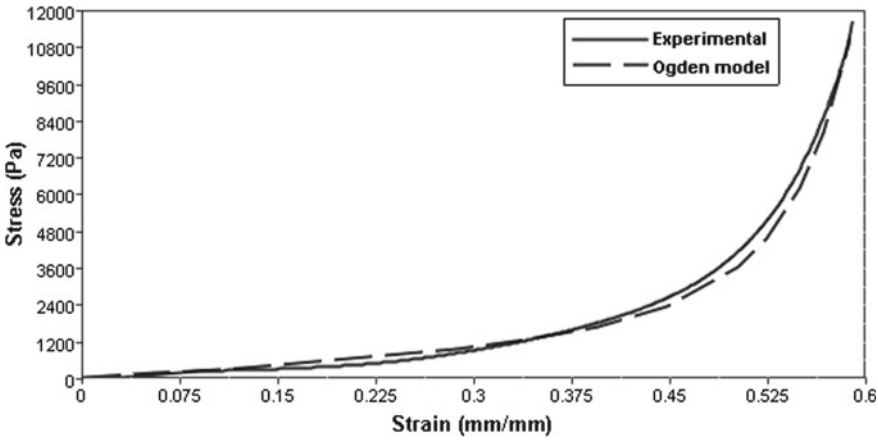

Fig. 5.11 Comparison of experimental and simulation stress–strain curves for compression test on latex foam

5.5 Conclusions

The dynamic response of pin-core natural latex open-cell polymer foam is determined by conducting drop tower impact experiments on the foam. Simulations of the drop tower experiments are performed with LS-DYNA, and good agreement is obtained for the force–time history derived from the experiments and simulation. Further, static uniaxial compression tests were carried out on the foam using universal testing machine (UTM). The compression test data were analyzed to determine the Ogden hyper-elastic material model parameters for the foam. In addition, numerical simulations of the uniaxial static compression tests on the foam were done using ADINA code, and good agreement was found between the test data and simulation results for the uniaxial compression stress–strain response. Furthermore, the effect of the water on the uniaxial compressive behavior of water-saturated open-cell latex polymer foam is demonstrated experimentally.

References

1. Ashby, M.F., Evans, A.G., Fleck, N.A., Gibson, L.J., Hutchinson, J.W., Wadley, H.N.G.: Metal Foams: A Design Guide. Butterworth-Heinemann, Oxford (2000)
2. Gibson, L.J., Ashby, M.F.: Cellular Solids: Structure and Properties, 2nd edn. Cambridge University Press, Cambridge (1999)
3. Venkataramana, K., Singh, R.K., Deb, A., Bhasin, V., Vaze, K.K., Kushwaha, H.S.: Blast protection of infrastructure with fluid-filled cellular polymer foam. In: 11th International Symposium on Plasticity and Impact Mechanics (IMPLAST-2016), IIT New Delhi, 11–14 Dec 2016. Proc. Eng. **173**, 547–554 (2017)
4. Venkataramana, K., Singh, R.K., Deb, A., Bhasin, V., Vaze, K.K., Kushwaha, H.S.: Numerical simulation of blast wave mitigation using foam impregnated with water. In: DAE BRNS Symposium on Multiscale Modeling of Materials and Devices (MMMD-2014), BARC, Mumbai, 30 Oct–02 Nov 2014
5. ADINA (Automatic Dynamic Incremental Nonlinear Analysis) v 9.2, ADINA R&D, Inc., Watertown, MA 02472, USA
6. LS-DYNA v971, Livermore Software Technology Corporation, Livermore, CA, USA
7. Dawson, M.A.: Composite plates with a layer of fluid-filled, reticulated foam for blast protection of infrastructure. Int. J. Impact Eng. **36**(10–11), 1288–1295 (2009)
8. Yost, A.L.: Fluid-filled helmet liner concept for protection against blast-induced traumatic brain injury. , Masters Thesis, Mechanical Engineering, Massachusetts Institute of Technology, Cambridge, MA (2012)
9. Goel, R.: Study of an advanced helmet liner concept to reduce TBI: experiments and simulation using sandwich structures. Masters thesis, Aeronautics and Astronautics, Massachusetts Institute of Technology. Cambridge, MA (2011)
10. Christou, G.A.: Development of a helmet liner for protection against blast induced trauma. Masters thesis, Aeronautics and Astronautics, Massachusetts Institute of Technology, Cambridge, MA (2010)
11. Venkataramana, K.: Blast effects on mild steel plates and blast protection using fluid-filled polymer foam. Ph.D. thesis, Indian Institute of Science (IISc), Bengaluru, May 2017
12. Rani, J.: Latex foam. In: Eves, D. (ed.) Handbook of Polymer Foams. Rapra Technology Limited, Shawbury, Shrewsbury, Shropshire, UK (2004). http://www.rapra.net, ISBN: 1-85957-388-6

13. MM foam Ltd., Chennai, Tamil Nadu, India. www.mmfoam.com
14. LS-DYNA Keyword Reference Manual, Vol-2, Material Models, Livermore Software Technology Corporation (LSTC), Livermore, CA (2013)
15. ASTM-D3574-11: Standard test methods for flexible cellular materials—slab, bonded, and molded urethane foams. Test C—compression force deflection test. ASTM International (2003)
16. ADINA Theory and Modeling Guide. vol. 1, ADINA Solids and Structures. ADINA R&D Inc., MA, USA